*Korean J. Chem. Eng.*, 33(4), 1296-1304 (2016)
DOI: 10.1007/s11814-015-0261-1

pISSN: 0256-1115
eISSN: 1975-7220

# Continuous cadmium removal from aqueous solutions by seaweed in a packed-bed column under consecutive sorption-desorption cycles

**Seyed Ali Jafari† and Abbas Jamali**

Department of Environment, Persian Gulf Research Institute, Persian Gulf University, 75169, Bushehr, Iran
(*Received 13 August 2015 • accepted 26 November 2015*)

**Abstract**−Packed-bed column process efficiency for cadmium adsorption from aqueous solution was investigated under different bed heights (2.6 to 7.5 cm) and feed flow rates (15 to 30 ml $min^{-1}$). The column was filled with brown seaweed, *Sargassum angustifolium*. Three simplified models, including Bed Depth Service Time, Thomas, and Yoon-Nelson were employed for describing the experimental breakthrough curves as well as achieving design parameters. Bed lifetime was also evaluated in several consecutive sorption-desorption cycles. Cadmium concentration of 0.005 mg $l^{-1}$, as a standard limit for potable water, was considered as the breakthrough concentration. The maximum column performance was achieved 81% at 7.5 cm bed length and flow rate of 15 ml $min^{-1}$. Indeed, increasing the bed height increased the sorption performance and service time, while increasing the feed flow rate had a negative effect. Maximum sorption capacity value remained almost constant by the bed height changes; however, increase in the feed flow rate slightly decreased it. The modeling results revealed that the Yoon-Nelson model was more accurate than Thomas for describing the experimental breakthrough data, especially at low flow rates. Column service time predictions were surprisingly achieved using the Bed Depth Service Time model even at extrapolations. 20% reduction in column adsorption efficiency was observed at the end of four consecutive sorption-desorption cycles; however, desorption efficiencies were achieved more than 99% in each cycle.

Keywords: BDST Model, Breakthrough, Cadmium, Packed-bed, Seaweed

## INTRODUCTION

Biosorption is a unique technique for heavy metal removal from aqueous solutions that has many advantages over traditional physicochemical methods. It is more economical than traditional methods, since it employs inexpensive materials such as seaweed, fungi, algae, agricultural wastes, and industrial fermentation by-products as biosorbent. These biomaterials are naturally environmentally friendly and do not leave chemical sludge at the end of the process. Biosorption has also been known for its high efficiency, especially at low metal concentrations, below 100 mg $l^{-1}$ [1,2]. Although traditional sorbent materials such as zeolites, activated carbon, silica and alumina have been used extensively in separation processes at large scale, they are expensive [3]. The cost of industrial scale processes should be reduced as far as possible by employing cheap and highly available biosorbent materials that would also be effective in metal sequestering during several sorption-desorption cycles [4]. The use of seaweeds as biosorbent for heavy metal removal is more economical in coastal cities because of their high production and high availability. It has also been proved that the metal uptake capacities of brown seaweeds, such as *Sargassum*, are much higher than other ones [5,6]. Separation based on adsorption-desorption cycles is widely used in various scales and with various purposes. The packed-bed column is usually preferred due to its effectiveness and a high sorption capacity [4,7]. The high metal concentration in influent is faced with fresh biosorbent where the highest driving force between the metal ions concentration in the water (Ci mg/*l*) and metal ions on the biomass surface (zero mg/*l*) occurs and leads to complete metal removal [7,8]. This phenomenon can also efficiently drive the processes even at very low levels of influent metal concentrations. Such a high driving force proceeds to the end of the bed and makes it possible to achieve a high purification in a single step [4]. Thus packed-bed column biosorption, unlike the batch one, is a practical application of heavy metal removal as the sorbent capacity is efficiently utilized and results in better quality of the effluent [9]. The *Sargassum* biomass has high metal sorption capacity besides being suitable for column operation since it does not swell and therefore does not cause operational problems such as clogging and pressure drop.

In the present study, cadmium removal from aqueous solutions was investigated using a packed-bed column filled with dried seaweed, *Sargassum angustifolium*. This research was carried out in Bushehr city, Iran, on September 2014. The variation in the main design parameters such as bed height and feed flow rate was examined on the adsorption process efficiency. Thomas, Yoon-Nelson, and Bed Depth Service Time (BDST) models were employed to describe the experimental breakthrough curves in order to obtain some design parameters, including mass transfer rate and maximum adsorption capacity as well as prediction of service time. The biosorbent lifetime was also evaluated in several consecutive sorption-

†To whom correspondence should be addressed.
E-mail: sajafari.pgrsc@yahoo.com

desorption cycles.

## MATERIALS AND METHODS

### 1. Biomass

The preliminary study revealed that *Sargassum angustifolium* had better cadmium sorption capacity compared to other studied seaweeds [10]. It was harvested from Bushehr coastal waters, Persian Gulf, Iran, and washed several times with tap water and 0.1 M HCl to remove salt and sands followed by rinsing with distilled water until the pH of the wash became neutral. It was then dried in a conventional oven at 60 °C for 48 hrs. Dried biomass in size between 0.5 to 0.7 mm was employed in packed-bed column for continuous cadmium removal from aqueous solutions.

### 2. Column Specification

Continuous-flow sorption experiments were conducted in a glass column with an internal diameter of 2.5 cm and 20 cm height. Wall effects could influence the shape of the breakthrough curve. To avoid such effect, the ratio of column diameter to particle diameter is recommended to be higher than 10 [11]. This was in compliance with the present study. A 3 cm height of glass beads (2 mm in diameter) was placed at top and bottom of the bed in order to pack the biomass as well as to provide a uniform inlet flow of the solution into the column. A 0.3 mm stainless sieve was placed between glass beads and bed to prevent biomass loss and bed movement through the glass beads (Fig. 1). An upward flow with constant flow rate was pumped through the column using a peristaltic pump and sampling was done at the column outlet.

### 3. Continuous-flow Sorption Experiments

All chemicals were of analytical grade and purchased from Merck.

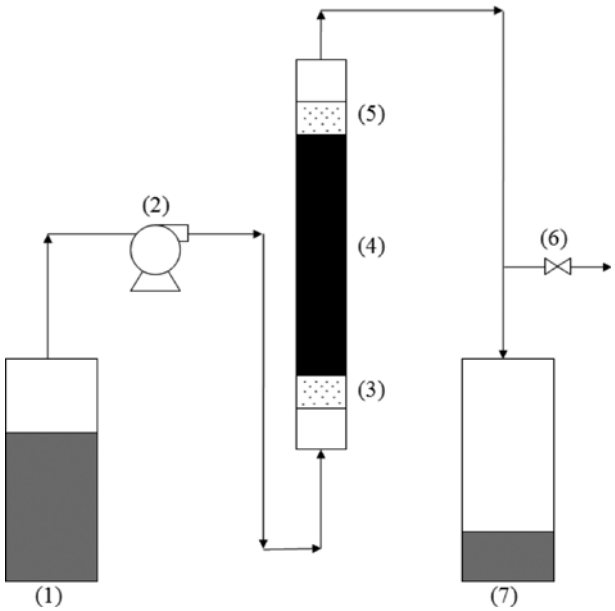


**Fig. 1. Packed-bed column process schematic.**

(1) Feed reservoir
(2) Peristaltic pump
(3) Bottom glass beads
(4) Column bed
(5) Top glass beads
(6) Sampling valve
(7) Effluent storage

The feed cadmium solution was prepared by dissolving the required quantity of cadmium salt ($CaCl_2$) in distilled water. Based on the batch preliminary study, the best pH value for cadmium biosorption by *Sargassum angustifolium* was obtained at 6 [10]. Therefore, the pH of the feed solution was initially adjusted to 6 by 0.1 M NaOH or 0.1 M $HNO_3$. All the experiments were at room temperature, 28-29 °C.

A peristaltic pump was used to pump upward the 65 mg $l^{-1}$ cadmium solution. The effects of three different bed heights of 2.6, 4.9 and 7.5 cm as well as feed flow rates of 15, 20 and 30 ml $min^{-1}$ were assessed on column performance. A desired bed height was achieved by known quantities of 4, 8 and 12 g biomass, respectively. Sampling was done at the column effluent at different time intervals. Then it was analyzed for cadmium residual concentration using a flameless atomic absorption spectrophotometer (PG instruments, AA500, England).

Plotting the effluent metal concentration or effluent to influent cadmium concentrations ratio versus time gives a sigmoid shape profile, the breakthrough curve. Some blank runs were also conducted using the same mass of glass beads in the column without any biosorbents to evaluate the effect of glass beads on the effluent cadmium concentration.

### 4. Bed Regeneration Experiments

The $Cd^{2+}$ biosorption process was stopped when the effluent cadmium concentration reached the influent one--where the bed is saturated and is no longer effective. It is essential to regenerate the saturated bed for reuse in several cycles due to economic reasons [12]. Although higher eluent concentration increases the regeneration efficiency, it adversely affects adsorbent structure as well as increasing the operating cost. It is reported that 1% $CaCl_2$ solution acidified to pH 3 by 1 M HCl is a proper regenerant with high elution efficiency and low biomass weight loss [7,9,13]. The upward flow with the rate of 40 ml $min^{-1}$ was considered for regeneration process upon bed saturation. The regenerated bed was reused for the next cycles. The pH and cadmium concentration in effluent was recorded at specific time intervals, and the process was stopped when no cadmium ion was observed in the effluent. After each regeneration process, the bed was well washed with distilled water to send out trapped calcium and proton ions in the bed and neutralize the final pH.

The plot of effluent cadmium concentration versus time in desorption experiments is called elution curve. The sorption-desorption experiments were continued for four consecutive cycles to evaluate the rates of biomass destruction, drop in metal removal efficiency and biomass sorption capacity per cycle.

### 5. Column Data Analyzing

Various parameters can be used to characterize the performance of a packed-bed column, including the length of Mass Transfer Zone (MTZ), slope of the breakthrough curve, metal uptake capacity, and removal efficiency [14]. The breakthrough time, $t_b$, is that at which the metal concentration in the effluent reaches a predetermined concentration or recommended limit. In the present work, the cadmium concentration of 0.005 mg $l^{-1}$ was considered for $t_b$ as the quality standard for potable water [15,16]. In reality, the adsorption process should be stopped at this point and desorption should be started immediately. However, at laboratory scale, the

complete breakthrough curve is needed to evaluate the dynamic response of biosorption column [14]. The point that the effluent metal concentration becomes equal to the influent one is the bed exhaustion time, $t_e$, after which the bed is no longer effective. In the present work, this value was considered as 95% of the initial cadmium concentration: 61.75 mg $l^{-1}$. The MTZ, the area between gradually saturated sorbent to fresh section, is evaluated by subtracting $t_b$ from $t_e$ and the metric length of MTZ can be approximately calculated by Eq. (1):

$$L_{min} = L\left(1 - \frac{t_b}{t_e}\right) \quad (1)$$

where L is the bed depth (cm) and $L_{min}$ is the length of adsorption zone (cm) which is also called minimum or critical bed length [7]. This length signifies the minimum bed height required to appear the breakthrough concentration at time zero [4]. The shape and slope of breakthrough curve from $t_b$ to $t_e$, dc/dt (difference in metal concentration divided by difference in time) is also used to characterize the performance of a column biosorption. A steep curve with short MTZ is always favored because it implies a longer service time and greater use of the sorbent [14].

The metal mass trapped in the bed, $m_{ad}$ (mg), is equal to the area above the breakthrough curve (C versus t), which is obtained by the numerical integration multiplied by the volumetric flow rate [9]. Dividing this parameter by the sorbent mass, M (g), gives the biomass uptake capacity, Q (mg $g^{-1}$). This corresponds to a point on the equilibrium isotherm and the influent concentration in the column corresponds to the final equilibrium concentration [7].

Total mass of the metal passed through the column, $m_t$ (mg), can be calculated by Eq. (2):

$$m_t = C_i F t_e \quad (2)$$

where F is the volumetric flow rate ($l$ $min^{-1}$) and $C_i$ is the influent metal concentration (mg $l^{-1}$). The column removal efficiency, $E_R$%, is then achieved as follows:

$$E_R\% = \frac{m_{ad}}{m_t} \times 100 \quad (3)$$

The metal mass desorbed, $m_d$ (mg), is calculated from the area below the elution curve (C versus t) multiplied by the volumetric flow rate. The elution efficiency, $E_{el}$%, can be achieved from Eq. (4):

$$E_{el}\% = \frac{m_d}{m_{ad}} \times 100 \quad (4)$$

where $m_{ad}$ is the metal mass trapped in the bed from the previous sorption cycle. In addition, the peak time, $t_p$, and peak concentration, $C_p$, are key factors in elution curve. The concentration factor, CF, is achieved by dividing $C_p$ by $C_i$ [15].

The rate of decreasing sorption performance of the bed during consecutive sorption-desorption cycles is called the life factor, which can be calculated in terms of the critical bed length as the following linear relationship [7]:

$$L_{min,i} = L_{min,0} + K_{lf}(i-1) \quad (5)$$

where $L_{min,i}$ and $L_{min,0}$ are the critical bed length at cycle and the initial critical bed length or intercept (cm), respectively, i is number of cycles and $K_{lf}$ is bed life factor (cm $cycle^{-1}$) obtained from the slope of plot of $L_{min,i}$ versus (i−1).

**6. Modeling**

Packed-bed column modeling can help to calculate some characteristic or design parameters as well as to predict the breakthrough curve behavior for scale-up purposes and performance comparison. Many models have been developed to fulfill these purposes [17]. The packed-bed column process is very complex and several factors, including axial dispersion, sorption kinetics, mass transfer, and intraparticle diffusion resistances, should be considered to have a reliable and perfect model. Solving such a complex model requires a series of non-linear partial differential equations [18]. Alternatively, simplified semi-empirical models such as Bed Depth Service Time (BDST), Thomas, and Yoon-Nelson have frequently been employed for describing the experimental breakthrough curve data [9,15,18-20]. These models are reliable for achieving some design parameters using experimental data; however, they suggest some simplifications that are usually not valid in reality. Nonetheless, using these simplified models is easier than solving complicated mathematical equations [18]. In addition, these models are useful for quantitatively assessing the effects of main system variables including bed height and feed flow rate on the column dynamics [20]. A nonlinear least-squares method was employed using MATLAB software to attain the best fit and obtain all the model parameters.

The Thomas model is the most widely used model to fit the experimental breakthrough curve data [21]. This model has the following nonlinear form of Eq. (6):

$$\frac{C}{C_i} = \frac{1}{1 + \exp[(K_{Th}/F)(QM - C_i tF)]} \quad (6)$$

where C and $C_i$ are the effluent and influent cadmium concentrations (mg $l^{-1}$) respectively, $K_{Th}$ is Thomas rate constant ($l$ $mg^{-1}$ $min^{-1}$) and Q is the maximum biosorption capacity (mg $g^{-1}$). This is a key parameter that is required in design. The main model deficiency appears when the variable t is zero, then the term $C/C_i$ becomes equal to a constant value, contrary to reality [14,18].

The coefficient of determination, $R^2$, was used as a criterion to evaluate the proximity of the observed and predicted results. However, a close value of $R^2$ to 1 does not necessarily imply that the regression model is a good one [2]. So, the absolute average deviation (AAD) was also considered along with $R^2$ to assess the accuracy of data fitting by the proposed model. AAD is calculated by Eq. (7) as follows:

$$AAD = \frac{\sum_{j=1}^{n}[(C/C_i)_{exp,j} - (C/C_i)_{pred,j}]}{n} \times 100 \quad (7)$$

where n is the number of data points and subscripts "exp" and "pred" referring to experimental and predicted values by the model, respectively.

Yoon-Nelson model is based on the assumption that the rate of decrease in the probability of adsorption for each adsorbate molecule is proportional to the probability of adsorbate adsorption and the probability of adsorbate breakthrough on the adsorbent [21,22]. This model has been frequently used for predicting breakthrough

curves [19]. The nonlinear form of the Yoon-Nelson model is presented in Eq. (8) as follows [14]:

$$\frac{C}{C_i}=\frac{\exp(K_{YN}t-K_{YN}\tau)}{1+\exp(K_{YN}t-K_{YN}\tau)} \quad (8)$$

where $K_{YN}$ is the Yoon-Nelson model rate constant ($min^{-1}$) and $\tau$ is the time that $C/C_i$ is equal to 0.5 (min).

The unknown parameters, $K_{YN}$ and $\tau$, are achieved by using direct fitting of the model to the experimental data by the nonlinear least-squares method.

The BDST is a simple model for predicting the relationship between bed height, L, and service time, t, in terms of feed flow rates, process concentrations and adsorption parameters [9]. The main advantage of the BDST model is that it can predict the slope for any unknown flow rates with a known slope at a given flow rate [4,23]. This fact reduces time-consuming and repetitive experiments [20]. Many researchers have used this model for breakthrough curve analyzing [9,15,18,23]. The equation can be expressed as:

$$t_b=\frac{N_0L}{C_i\upsilon}-\frac{1}{K_aC_i}\ln\left(\frac{C_i}{C_b}-1\right) \quad (9)$$

where $t_b$ is breakthrough time (h), $C_i$ and $C_b$ are the influent and breakthrough metal concentrations (mg $l^{-1}$), respectively, $N_0$ is sorption capacity of bed per unit bed volume (mg $l^{-1}$), is linear or superficial velocity calculated by dividing the flow rate by the column section area (cm $h^{-1}$), and $K_a$ is the rate constant ($l$ $mg^{-1}$ $h^{-1}$), which characterizes the rate of solute transfer from the fluid phase to the solid phase [9]. The slope of the plot of $t_b$ versus L at a fixed flow rate represents the time required for the adsorption zone to travel a unit length through the bed and gives $N_0$. The value of $K_a$ is achieved from the intercept of this plot. However, the BDST model includes some limitations, such as the symmetry assumption of the breakthrough curves that is not true in reality [18]. In addition, the model ignores the intraparticle mass transfer resistance and the external film resistance [22].

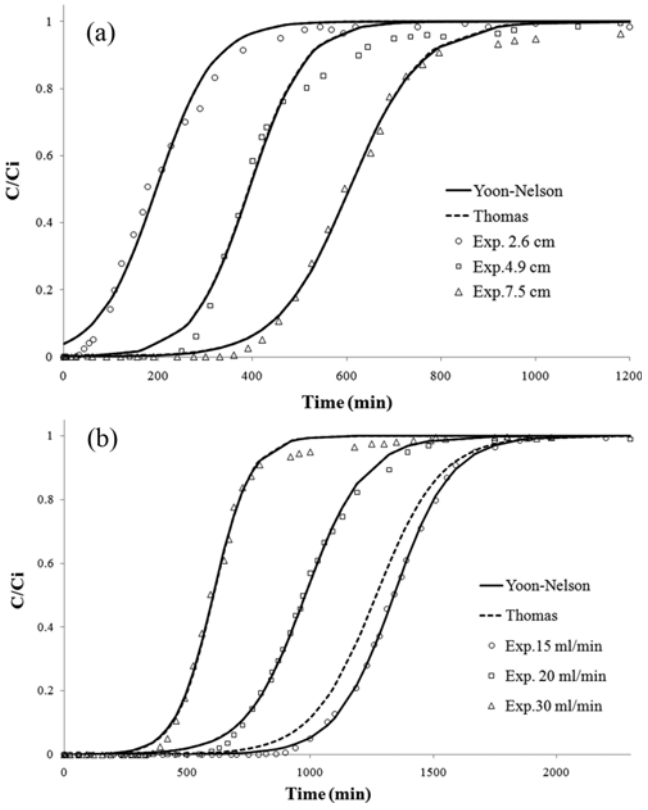


**Fig. 2. Packed-bed column performance at (a) several bed heights of 2.6 (○), 4.9 (□) and 7.5 (△) cm and (b) at several flow rates of 15 (○), 20 (□) and 30 (△) ml $min^{-1}$. The solid circles (●) and dashed lines (---) show predicted breakthrough curves using the Yoon-Nelson and Thomas models, respectively.**

## RESULTS AND DISCUSSION

### 1. Effect of Bed Height

The effect of bed heights of 2.6, 4.9 and 7.5 cm were evaluated on biosorption column performance at a fixed flow rate of 30 ml $min^{-1}$ and influent cadmium concentration of 65 mg $l^{-1}$.

Table 1 reports the obtained data by increasing bed height. The metal mass trapped in the bed, $m_{ad}$, increased from 409 to 1,219 mg by increase in bed height in the column from 2.6 to 7.5 cm. It was due to the increase in the amount of adsorbent used in the bed, which increases the total sorption area through the bed. However, the metal sorption capacity of *S. angustifolium* was obtained roughly constant by bed height. This is in accordance with the results obtained by Lodeiro et al. [18]. The column removal efficiency, as system performance, increased from 45.6 to 62.5% by increasing in bed height from 2.6 to 7.5 cm.

Fig. 2(a) shows that increasing the bed height postponed the breakthrough and exhaustion times, increased the critical bed length, decreased the MTZ slope and broadened it as more surface area and more binding sites were available for metal sorption [22,24].

It is also clear from Fig. 2(a) that the experimental breakthrough curves exhibit an asymmetric shape. It means that the experimental data rapidly detached from the horizontal axis (a sharp leading edge), but in the end it was gradually attached to the line $C_e/C_i=1$

**Table 1. Breakthrough curves data obtained at various feed flow rate and bed height of a packed bed column for cadmium biosorption by *Sargassum angustifolium***

| Bed height (cm) | Flow rate (ml $min^{-1}$) | $m_{ad}$ (mg) | $m_t$ (mg) | Q (mg $g^{-1}$) | $t_b$ (hr) | $t_e$ (hr) | dc/dt | $L_{min}$ (cm) | $E_R$% |
|---|---|---|---|---|---|---|---|---|---|
| 2.6 | 30 | 409.35 | 897 | 102.34 | 16 | 460 | 0.162 | 2.41 | 45.64 |
| 4.9 | 30 | 812.88 | 1365 | 101.61 | 170 | 700 | 0.140 | 3.79 | 59.55 |
| 7.5 | 30 | 1219.42 | 1950 | 101.82 | 325 | 1000 | 0.106 | 5.06 | 62.53 |
| 7.5 | 20 | 1295.84 | 1813 | 107.99 | 490 | 1395 | 0.092 | 4.87 | 71.46 |
| 7.5 | 15 | 1304.59 | 1628 | 108.72 | 710 | 1670 | 0.068 | 4.31 | 80.91 |

**Table 2. Thomas and Yoon-Nelson model parameters obtained by nonlinear fit of the breakthrough data. AAD% was presented for comparing models accuracy on data fitting**

| Bed height (cm) | Flow rate (ml min$^{-1}$) | Thomas | | | | | Yoon-Nelson | | | | |
|---|---|---|---|---|---|---|---|---|---|---|---|
| | | $Q_{exp}$ (mg g$^{-1}$) | $Q_{model}$ (mg g$^{-1}$) | $K_{Th}$ ($l$ mg$^{-1}$ min$^{-1}$) | $R^2$ | AAD% | $\tau_{exp}$ (min) | $\tau_{model}$ (min) | $K_{YN}$ (min$^{-1}$) | $R^2$ | AAD% |
| 2.6 | 30 | 102.34 | 95.66 | 0.00025 | 0.993 | 3.26 | 178 | 196 | 0.0163 | 0.993 | 3.26 |
| 4.9 | 30 | 101.61 | 95.62 | 0.00026 | 0.992 | 3.27 | 385 | 393 | 0.0168 | 0.992 | 3.29 |
| 7.5 | 30 | 101.82 | 98.36 | 0.00020 | 0.998 | 1.68 | 595 | 605 | 0.0131 | 0.998 | 1.68 |
| 7.5 | 20 | 107.99 | 106.15 | 0.00013 | 0.998 | 1.24 | 970 | 979 | 0.0082 | 0.998 | 1.24 |
| 7.5 | 15 | 108.72 | 103 | 0.00012 | 0.983 | 4.22 | 1340 | 1338 | 0.0085 | 0.999 | 0.52 |

(a broad trailing edge). This slow approach of $C_e/C_i$ towards 1 is usually called "tailing." Increasing the bed height also increased the tail and decreased the sharpness of the edges, especially the trailing edge. This behavior may be explained either by the existence of mass transfer limitation or flow non-idealities [25]. Since the flow direction in the column was adjusted upward, a plug flow can be assumed with minimal or negligible non-idealities. Therefore, hat mass transfer limitation could be the most probable factor that affects the tailing of breakthrough curve. As Cooney [26] claimed, the tailing of a breakthrough curve is commonly observed in liquid phase sorption where intraparticle diffusion is the rate-limiting transport process. This phenomenon becomes dominant at the end part of the process where the bed is semi-saturated, the metal ions are aggregated on the biomass surface, and other ions in the solution try to diffuse into the particles. This extends the bed completely to saturation and appears as a tail.

**2. Effect of Feed Flow Rate**

Flow rate is an important factor that affects the column performance. When the intraparticle diffusion controls the process, a slower flow rate could be more favorable. However, if the external mass transfer (i.e., metal ion transfer from bulk solution toward the surface of the adsorbent) controls the biosorption, the process should be managed with higher flow rate since it decreases the external and film mass transfer resistance: that is, a very thin mass transfer layer around the particle that resists against ion attachment to the surface of the adsorbent [14].

The effect of feed flow rate in the range of 15 to 30 ml min$^{-1}$ was studied on the packed-bed column performance at a fixed bed height of 7.5 cm and a fixed influent cadmium concentration of 65 mg $l^{-1}$. As can be seen from Table 1, increasing the feed flow rate from 15 to 30 ml min$^{-1}$ decreased the adsorption capacity of the bed from 108 to 101 mg g$^{-1}$ which can be attributed to less residence time of metal ions in the column [22,27]. Also, increasing the feed flow rate increased the total metal mass passed through the column, $m_t$, while decreasing the metal mass trapped in the bed, $m_{ad}$. This led to a significant reduction in column efficiency from 80.92 to 62.53%. It agrees with the findings of Zulfadhly et al. [23] and Vijayaraghavan et al. [9]. According to Table 1, the breakthrough curve became steeper (i.e., the dc/dt value increased) and the breakthrough and exhaustion times decreased by increasing the feed flow rate or velocity through the bed. It can also be seen in Fig. 2(b). As expected, increasing the flow rate from 15 to 30 ml min$^{-1}$ increased the depth of adsorption zone or critical bed length from 4.31 to 5.06 cm (Table 1). So, at higher flow rates the metal ions in the column do not have enough time to diffuse into the biomass pore or to bind to the surface ligands. Therefore, more bed height is needed to adsorb the same amount of metal ion. The same results were found in other literature [20,23,28].

The blank experiments revealed that the glass beads had no influence on cadmium removal and the effluent cadmium concentration did not significantly change over time (data not shown).

**3. Modeling**

The breakthrough curves obtained in the present experiments need to be examined quantitatively. A valid model should be able to well describe the experimental breakthrough curve data and give the reliable design parameters [29]. Sometimes the model should be employed to predict the effects of main system variables on the column dynamics.

3-1. Thomas Model

The dashed lines in Fig. 2(a) and (b) are the predicted breakthrough curves by Thomas model. The estimated parameters $K_{Th}$ and Q by the least-squares method are listed in Table 2. The high coefficient of determination (higher than 0.983), low AAD (lower than 4.22), and proximity values of $Q_{exp}$ and $Q_{model}$ at all studied flow rates and bed heights imply a reliable Thomas model for data fitting. However, a significant mismatch with the experimental data was observed at edges as well as at low flow rate of 15 ml min$^{-1}$. The existing error values could be due to the asymmetry profile of the experimental breakthrough curves [20]. In addition, the Thomas model assumes no axial dispersion through the system [22,29].

Increasing the $K_{Th}$ value with flow rate ($R^2$=0.948) implies that the liquid mass transfer is directly related to the feed flow rate [29].

3-2. Yoon-nelson Model

The obtained parameters in all conditions examined as well as $R^2$ and AAD% values are reported in Table 2. The predicted values for $\tau$ are quite close to the experimental ones. In addition, solid lines in Fig. 2(a) and (b) illustrate good data fitting by Yoon-Nelson model. Although the predicted breakthrough curves by Thomas and Yoon-Nelson models are considerably close to each other and even fall on each other at flow rates more than 20 ml min$^{-1}$, Yoon-Nelson seems to be a more appropriate model for breakthrough prediction, especially at low feed flow rates. The Thomas model has a larger AAD% value for data fitting at 15 ml min$^{-1}$ than the Yoon-Nelson model, as reported in Table 2. In addition, the other AAD% values at low flow rate of 15 ml min$^{-1}$ and other bed heights of 2.6 and 4.9 cm suggest the Yoon-Nelson model is more

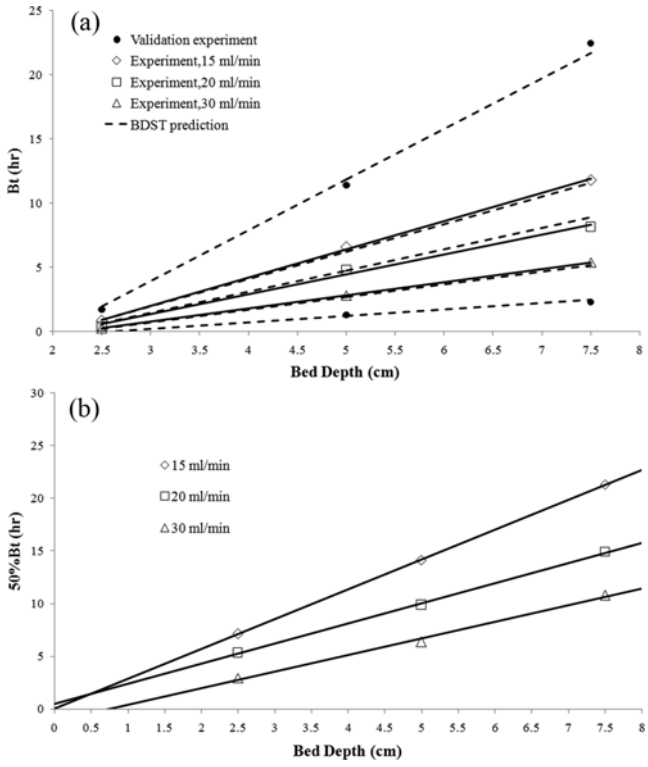


**Fig. 3. The experimental bed depth versus service time at several flow rates of 15 (◇), 20 (□) and 30 (△) ml min$^{-1}$ and the predicted relationships (---) using the BDST model. The solid circles (●) show the validation experiments at flow rates of 5 and 40 ml min$^{-1}$.**

preferable than the Thomas model. These values were obtained as 1.07 and 0.95% for Yoon-Nelson model and 3.05 and 3.24% for Thomas model at bed heights of 2.6 and 4.9 cm, respectively.

3-3. The BDST Model

The analysis of breakthrough curve was also done using the BDST model. The solid lines in Fig. 3(a) illustrate the linear relationship between the experimental service time and bed depth at flow rates of 15, 20 and 30 ml min$^{-1}$. The high values of coefficient of determination (higher than 0.99) indicate the validity of BDST model. By letting t=0 and solving for L in Eq. (9), the minimum bed depth, $L_{min}$, was obtained. This indicates the shortest possible bed length needed at a given flow rate to obtain the breakthrough concentration at time zero [18].

Table 3 shows the obtained parameters from BDST model at studied flow rates. The $L_{min}$ and $K_a$ parameters showed linear relationship with flow rate with significantly high $R^2$ values of 0.994 for both. However, values showed no dependency on change in the flow rate. The value increased from 0.032 to 0.063 $l$ mg$^{-1}$ h$^{-1}$ as the flow rate increased from 15 to 30 ml min$^{-1}$. This dependency means that at low operation times, until breakthrough time, the mass transfer in the fluid phase controls the rate of solute transfer from the fluid phase to the solid phase [18]. Increasing the feed flow rate decreases the external and film mass transfer resistance and consequently provides faster ion transfer from the solution toward the biomass surface ligands [14]. The same trend was found by Naddafi et al. [29] for lead and cadmium biosorption and by Lodeiro et al. [18] for cadmium biosorption by protonated *Sargassum* in a continuous packed bed column.

Predicted values are other important results that can be explained from Table 3. Dashed lines in Fig. 3(a) were plotted using the predicted slopes and intercepts by the BDST model. To predict any data using the BDST model, it seems to be necessary to achieve two separate specific relationships between both known slopes and known intercepts at different studied flow rates. These separate relationships for slope and intercept can extrapolate any other unknown slopes and intercepts at unknown flow rates. Although the intercept term in Eq. (9) is not flow rate dependent, note that the data presented in Table 3 show that the experimental intercept is flow rate dependent and increased by increase in flow rate. All other obtained results and provided figures by Mukhopadhyay et al. [4], Volesky and Prasetyo [15], and Zulfadhly et al. [23] confirm this claim and even reveal that slope and intercept variations by flow rate are not linear. However, Vijayaraghavan and Prabu [22] have a contrary claim. They assume that the intercept term in BDST model does not change with flow rate and the new unknown slope is in a linear relation with a known slope. This claim is not applicable to the present study as well as to the results of other mentioned literature. Based on the present claim, some verification experiments were conducted at flow rates of 5 and 40 ml min$^{-1}$, out of the studied range, to assess the BDST model prediction for

**Table 3. BDST equation terms (slope and intercept) and the corresponding parameters**

| Flow rate (ml min$^{-1}$) | Run | $m_{ad}$ (mg) | Slope | Intercept | $R^2$ | $K_a$ ($l$ mg$^{-1}$ h$^{-1}$) | $N_0$ (mg $l^{-1}$) | $L_{min}$ (cm) |
|---|---|---|---|---|---|---|---|---|
| 15 | Main runs | Experiment | 2.19 | −4.54 | 0.999 | 0.0321 | 435.65 | 2.069 |
| 15 | | Predict | 2.13 | −4.41 | 1 | 0.0330 | 423.34 | 2.069 |
| 20 | | Experiment | 1.55 | −3.28 | 0.993 | 0.0445 | 410.49 | 2.115 |
| 20 | | Predict | 1.66 | −3.50 | 1 | 0.0416 | 438.56 | 2.114 |
| 30 | | Experiment | 1.03 | −2.31 | 0.999 | 0.0630 | 409.17 | 2.244 |
| 30 | | Predict | 0.98 | −2.22 | 1 | 0.0657 | 391.69 | 2.250 |
| 5 | Verification | Experiment | 4.04 | −7.95 | 0.988 | 0.0183 | 267.75 | 1.965 |
| 5 | | Predict | 3.95 | −7.88 | 1 | 0.0185 | 261.30 | 1.997 |
| 40 | | Experiment | 0.54 | −1.40 | 1[a] | 0.1061 | 35.48 | 2.562 |
| 40 | | Predict | 0.51 | −1.31 | 1 | 0.1112 | 33.81 | 2.565 |

[a]For two experimental points. Because, the critical bed length was higher than the bed height examined, 2.4 cm, at this flow rate

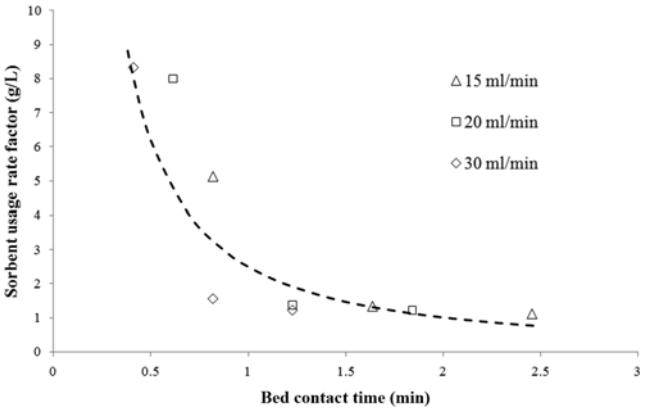


**Fig. 4. Effect of sorption column liquid residence time on specific usage of biosorbent *Sargassum angustifolium* at flow rates of 15 (△), 20 (□) and 30 (◇) ml min$^{-1}$.**

slopes and intercepts. Reliable results can be seen quantitatively in Table 3 and qualitatively in Fig. 3(a) by dashed lines and solid circles. Good consistency between the experimental and predicted values suggests the BDST as a successful model for predicting the service time under unknown flow rates without doing any additional experiments.

Passing the straight lines of bed depth versus 50% breakthrough curve through the origin could be another confirmation of the validity of BDST model [23]. It is when the intercept term in Eq. (9) is equal to zero. However, the failure of this linearization could be attributed to the complex mechanism of metal uptake by the biosorbent [23]. As depicted in Fig. 3(b), the lines almost pass through the origin, except for the highest flow rate of 30 ml min$^{-1}$. Lodeiro et al. [18] used similar validation for cadmium removal in a fixed-bed column by protonated *Sargassum muticum*.

Both the parameters, $N_0$ and $K_a$, are reflected in the sorbent usage rate factor, which is determined by dividing the mass of biosorbent in the column by the volume of solution treated up to the breakthrough time. The minimum value of this parameter is desired, and it can be achieved experimentally by plotting usage rate factor as a function of the bed contact time (bed volume/F), which represents the flow rate in the column [15,18]. According to Fig. 4, the optimal lowest sorbent usage rate was 1.12 g $l^{-1}$ which is in the region of low flow rates. This indicates that the ideal contact time in the column should not be less than 2.45 min in order to maintain the lowest usage rate, 1.12 g $l^{-1}$.

## 4. Consecutive Sorption-desorption Cycles

It is more attractive if the saturated biomass becomes regenerated and reused in another sorption cycles. It is also desired to retain the sorption efficiency in high levels during several sorption-desorption cycles.

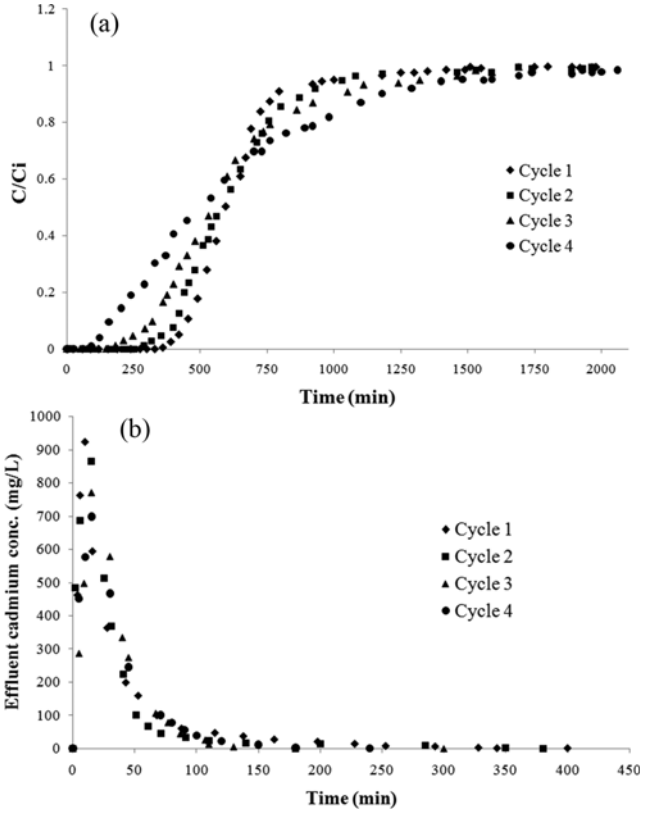


**Fig. 5. (a) The breakthrough and (b) the elution curves for four consecutive sorption-desorption cycles. Bed height of 7.5 cm, sorption flow rate of 30 ml min$^{-1}$, desorption flow rate of 40 ml min$^{-1}$, influent metal concentration of 65 mg $l^{-1}$, initial pH of 6 and 3 for sorption and desorption processes, respectively.**

In the present work, the bed sorption and desorption efficiencies were examined under four consecutive sorption-desorption cycles. All the breakthrough and elution curves are illustrated in Fig. 5(a) and (b), and the quantitative characterization of sorption-desorption cycles is summarized in Table 4.

Elution curves in Fig. 5(b) indicate that the metal concentration profile was initially raised to reach a peak value, $C_p$, and then gradually decreased to almost zero. Similar profiles were observed for all the cycles; however, the $C_p$ values decreased as the cycles progressed. According to Fig. 5(a), where all breakthrough curves are plotted in one diagram, the slope of breakthrough curve de-

**Table 4. Process parameters for four consecutive sorption-desorption cycles under feed flow rates of 30 and 40 ml min$^{-1}$ for sorption and desorption process, respectively**

| Cycle no. | $m_{ad}$ (mg) | Bed height (cm) | Q (mg g$^{-1}$) | $t_b$ (min) | $t_e$ (min) | dc/dt | $L_{min}$ (cm) | $C_p$ (mg $l^{-1}$) | $t_p$ (min) | CF | $E_R$% | $E_{El}$% |
|---|---|---|---|---|---|---|---|---|---|---|---|---|
| 1 | 1219 | 7.5 | 101.62 | 325 | 1000 | 0.106 | 5.06 | 924 | 10 | 14.22 | 62.53 | 99.73 |
| 2 | 1190 | 7.5 | 99.19 | 211 | 1030 | 0.091 | 5.96 | 865 | 15 | 13.32 | 59.26 | 99.65 |
| 3 | 1181 | 7.5 | 98.46 | 105 | 1325 | 0.061 | 6.90 | 771 | 15 | 11.87 | 45.90 | 98.89 |
| 4 | 1159 | 7.4 | 96.66 | 17 | 1480 | 0.048 | 7.41 | 699 | 10 | 10.76 | 40.19 | 99.48 |

creased from 0.106 mg $l^{-1}$ $min^{-1}$ in the first cycle to 0.048 mg $l^{-1}$ $min^{-1}$ at the end of the fourth cycle. The final slope was about half the first, as it can clearly be seen in the figure. Volesky et al. [7] reported the same trend after ten consecutive cycles. This can be attributed to surface ligand destruction by regenerant solution, which decreased the number of accessible binding sites for metal ions and caused the breakthrough point to appear much earlier at the effluent. Decrease in the metal mass adsorbed onto the biosorbent from 1,219 mg cadmium in the first cycle to 1,159 mg at the end of the fourth cycle was an evidence for surface ligands destruction. The metal uptake capacity also diminished from 101.6 to 96.7 mg $g^{-1}$ (Table 4). This decreased the removal efficiency from 62.5 to 40.2%. However, the elution efficiency, the area below the concentration-time profile in Fig. 5(b), was high (>98.8%) and roughly constant for all the cycles. The metal adsorption process is strongly dependent on the pervious desorption process. Prolonged contact time between acidified solution and the biosorbent during the regeneration process gradually disables the biosorbent.

According to Table 4, no significant change was observed in the bed height at the end of the fourth cycle. So it can be deduced that the loss of sorption efficiency, $E_R$%, or decrease in metal uptake capacity, Q, were not due to biosorbent decomposition, but due to sorbing sites inactivation whose accessibility becomes difficult for metal ions [14]. As Vijayaraghavan et al. [13] cited, acid solution could dissolve some surface ligands that may contribute to metal binding. In general, an elution process is usually fast compared to that of sorption. Thus, a high metal mass in a small elutant volume would be expected [14]. The complete metal elution was performed within 4 to 7 h. The CF values in Table 4 indicate that the initial metal solution was concentrated at 14.2, 13.3, 11.9, and 10.8 fold as the cycles progressed. In addition, these values were achieved during the first 10-15 min of contact for all cycles, $t_p$. The bed life factor was achieved at 0.799 cm $cycle^{-1}$ using Eq. (5) with $R^2$=0.985. The initial critical bed length, $L_{min,0}$, was also obtained, 5.14 cm. This value is very close to that obtained experimentally for the first cycle, 5.06 cm (Table 4).

## CONCLUSION

A packed-bed column is usually preferred for industrial scale adsorption processes due to its high sorption capacity. In this research, indigenous brown seaweed, *Sargassum angustifolium*, was employed as packing in a column for continuous cadmium removal from aqueous solutions. The effect of different bed heights and feed flow rates was evaluated on column efficiency. The maximum column efficiency was achieved 81% at the highest bed height, 7.5 cm, and the lowest feed flow rate, 15 ml $min^{-1}$. The experimental breakthrough curves were then fitted using nonlinear forms of Thomas and Yoon-Nelson models. Although the estimated design parameters by both models were in good agreement with the experimental ones, the Yoon-Nelson model was more appropriate for breakthrough prediction than the Thomas model, especially at low flow rates. The BDST model was also employed to describe the relationship between bed depth and service time at all the studied flow rates. In addition, this model was used to predict the service time in other unknown flow rates without doing any experiments. The BDST model was validated by great $R^2$ values (>0.99) at studied flow rates in the range of 15 to 30 ml $min^{-1}$. Furthermore, the good consistency between the experimental and predicted values in verification tests at outer flow rates of 5 and 40 ml $min^{-1}$ proved the ability of the BDST model for prediction and scale up. Note that the intercept term in the BDST model was not constant by change in feed flow rate. The bed sorption efficiency in four consecutive sorption-desorption cycles was evaluated and found to be a 20% reduction at the end of the fourth cycle. However, the desorption efficiency was high and almost constant as the cycles progressed, >98%. The biosorbent life factor was achieved at 0.799 cm $cycle^{-1}$. This method can be useful for valuable metal concentrating and sequestering for further use.

## ACKNOWLEDGEMENT

This research was done with the financial support of the Department of Research Affairs of Persian Gulf University and the laboratory facilities of Persian Gulf Research Institute.

The authors have declared no conflict of interest.

## REFERENCES

1. R. Say, A. Denizli and M. Yakup Arıca, *Bioresour. Technol.*, **76**, 67 (2001).
2. S. A. Jafari, S. Cheraghi, M. Mirbakhsh, R. Mirza and A. Maryamabadi, *CLEAN*, **43**, 118 (2015), DOI:10.1002/clen.201300616.
3. A. Hatzikioseyian, F. Mavituna and M. Tsezos, *Process Metallurgy*, **9**, 429 (1999).
4. M. Mukhopadhyay, S. B. Noronha and G. K. Suraishkumar, *Chem. Eng. J.*, **144**, 386 (2008).
5. M. A. Hashim and K. H. Chu, *Chem. Eng. J.*, **97**, 249 (2004).
6. J. Wang and C. Chen, *Biotechnol. Adv.*, **27**, 195 (2009).
7. B. Volesky, J. Weber and J. M. Park, *Water Res.*, **37**, 297 (2003).
8. G. Yan and T. Viraraghavan, *Bioresour. Technol.*, **78**, 243 (2001).
9. K. Vijayaraghavan, J. Jegan, K. Palanivelu and M. Velan, *Chemosphere*, **60**, 419 (2005).
10. S. A. Jafari, A. Jamali and A. Hosseini, *Korean J. Chem. Eng.*, **32**, 2053 (2015), DOI:10.1007/s11814-015-0013-2.
11. E. Worch, *Adsorption technology in water treatment: Fundamentals, processes, and modeling*, Walter de Gruyter (2012).
12. C. Zhu, Z. Luan, Y. Wang and X. Shan, *Sep. Purif. Technol.*, **57**, 161 (2007).
13. K. Vijayaraghavan, K. Palanivelu and M. Velan, *Process Biochem.*, **41**, 853 (2006).
14. K. Vijayaraghavan and Y. S. Yun, *Biotechnol. Adv.*, **26**, 266 (2008).
15. B. Volesky and I. Prasetyo, *Biotechnol. Bioeng.*, **43**, 1010 (1994).
16. Gh. Tolian, S. A. Jafari and S. Zarei, *Water Quality Research Journal of Canada*, **50**, 109 (2015), DOI:10.2166/wqrjc.2015.007.
17. G. Yan, T. Viraraghavan and M. Chen, *Adsorpt. Sci. Technol.*, **19**, 25 (2001).
18. P. Lodeiro, R. Herrero and M. E. Vicente, *J. Hazard. Mater.*, **137**, 244 (2006).
19. R. Senthilkumar, K. Vijayaraghavan, M. Thilakavathi, P. V. R. Iyer and M. Velan, *J. Hazard. Mater.*, **136**, 791 (2006).
20. K. H. Chu and M. A. Hashim, *J. Environ. Sci.*, **19**, 928 (2007).

21. E. Malkoc, Y. Nuhoglu and Y. Abali, *Chem. Eng. J.,* **119**, 61 (2006).
22. K. Vijayaraghavan and D. Prabu, *J. Hazard. Mater.,* **137**, 558 (2006).
23. Z. Zulfadhly, M. D. Mashitah and S. Bhatia, *Environ. Pollut.*, **112**, 463 (2001).
24. N. K. E. M. Yahaya, I. Abustan, M. F. P. M. Latiff, O. S. Bello and M. A. Ahmad, *Int. J. Eng. Technol.*, **11**, 248 (2011).
25 K H. Chu, *Chem. Eng. J.*, **97**, 233 (2004).
26. D. O. Cooney, *Chem. Eng. Commun.*, **110**, 217 (1991).
27. B. Y. Chen, C. Y. Chen, W. Q. Guo, H. W. Chang, W. M. Chen, D. J. Lee and J. S. Chang, *Bioresour. Technol.*, **160**, 175 (2014).
28. J. T. Nwabanne and P. K. Igbokwe, *Int. J. Appl. Sci. Technol.,* **2**, 106 (2012).
29. K. Naddafi, R. Nabizadeh, R. Saeedi, A. H. Mahvi, F. Vaezi, K. Yaghmaeian and S. Nazmara, *J. Hazard. Mater.*, **147**, 785 (2007).